Exp Brain Res (1987) 65: 582–592

Experimental Brain Research

Local precision of visuotopic organization in the middle temporal area (MT) of the macaque

T.D. Albright and R. Desimone

Department of Psychology, Green Hall, Princeton University, Princeton, NJ 08544, USA,
and Laboratory of Neuropsychology, National Institute of Mental Health, Bethesda, MD 20205, USA

Summary. The representation of the visual field in the middle temporal area (MT) was examined by recording from single neurons in anesthetized, immobilized macaques. Measurements of receptive field size, variability of receptive field position (scatter) and magnification factor were obtained within the representation of the central 25°. Over at least short distances (less than 3 mm), the visual field representation in MT is surprisingly orderly. Receptive field size increases as a linear function of eccentricity and is about ten times larger than in V1 at all eccentricities. Scatter in receptive field position at any point in the visual field representation is equal to about one-third of the receptive field size at that location, the same relationship that has been found in V1. Magnification factor in MT is only about one-fifth that reported in V1 within the central 5° but appears to decline somewhat less steeply than in V1 with increasing eccentricity. Because the smaller magnification factor in MT relative to V1 is complemented by larger receptive field size and scatter, the point-image size (the diameter of the region of cortex activated by a single point in the visual field) is roughly comparable in the two areas. On the basis of these results, as well as on our previous finding that 180° of axis of stimulus motion in MT are represented in about the same amount of tissue as 180° of stimulus orientation in V1, we suggest that a stimulus at one point in the visual field activates at least as many functional "modules" in MT as in V1.

Key words: Visual area MT – Receptive field size – Receptive field scatter – Magnification factor – Point-image size – Modular organization

Offprint requests to: T.D. Albright (address see above)

Introduction

Since Mountcastle's (1957) original description of the columnar organization of the somatosensory cortex, the concepts of columns and modules have been of fundamental importance in understanding the functional organization of the primary sensory cortices. In the visual system of primates, the striate cortex (V1) has been shown to contain alternating band-like ocular dominance columns and systematic arrays of orientation columns interspersed with non-oriented zones (Hubel and Wiesel 1963, 1974a; Livingstone and Hubel 1984). The relationship between the visual field map and the orientation and ocular dominance systems in V1 is such that one or more complete sets of orientation and ocular dominance columns are available to process information from any point in the visual field (Hubel and Wiesel 1974b; Dow et al. 1981). Striate cortex appears to consist of hundreds of such hypercolumns or modules.

Extrastriate cortex may also be organized in a modular fashion. The middle temporal visual area (MT), an area first described by Allman and Kaas (1971) in the owl monkey, has a high proportion of directionally selective cells (Zeki 1974; Baker et al. 1981; Van Essen et al. 1981; Albright et al. 1984). We found that MT, which receives a direct projection from V1, contains a columnar system for the axis of stimulus motion that is similar in many ways to the orientation system of V1 (Albright et al. 1984). Even the scales of the columnar representations are similar: 180° of axis of stimulus motion in MT and 180° of stimulus orientation in V1 are each represented in a minimum of about 400–500 μm of cortex (Hubel and Wiesel 1974a) [Blasdel and Salama (1986) suggest a somewhat larger value in V1]. However, a number of striking differences in the visuotopic organization of MT and V1 have been reported. MT is only about one-tenth the size of V1, has much larger receptive

fields, and has a visual field map that has been described as "crude and essentially quadrantic" (Dubner and Zeki 1971), and showing "substantial irregularities in the detailed pattern of topographic organization" (Van Essen et al. 1981). Such differences suggest that points in the visual field may be represented in a fundamentally different fashion in MT than they are in V1, and the concept of a complete module being available to process information from any point in the visual field may not apply. To better understand the differences and similarities between MT and V1, we have examined the precision of visuotopic organization, magnification factor, receptive field size, scatter, and point-image size in MT and compared the results to those found by others in V1.

We report here that the visuotopic organization of MT is highly systematic, at least on a local scale, confirming the earlier claims of Gattass and Gross (1981). The scatter in receptive field position is approximately equal to one-third of the receptive field size, similar to the relationship that has been found in V1 (Dow et al. 1981). We also found that point-image size in MT, or the diameter of the cortical region activated by a single point in the visual field, is sufficiently large to encompass at least one complete set of axis-of-motion columns at all eccentricities. Thus, in MT as in V1, a full set of neural machinery is available to process the information from any given point in the visual field.

Methods

Animal preparation and maintenance

Four *Macaca fascicularis* weighing between 4 and 5 kg were each recorded from 7–9 times over a 4-week period. One week prior to the first recording session, a 3 cm diameter stainless steel cylinder and a head bolt oriented in the stereotaxic planes were affixed to the animal's skull with screws and dental acrylic. The exposed bone inside the cylinder was sealed with a thin layer of acrylic and a stainless steel cap was then placed on the cylinder. Surgical procedures were performed under ketamine (Ketaset) anesthesia, using an initial dose of 35 mg/kg and supplemented with 50 mg as necessary; 2.5 mg of Valium were also used.

On the day of the recording session the animal was given a restraining dose of ketamine (4 mg/kg) and then anesthetized with halothane in a 7 : 3 mixture of nitrous oxide and oxygen. The head was held firmly in a stereotaxic apparatus by means of the head bolt and a specially designed holder attached to the apparatus. (This method eliminates the potentially painful pressure of ear and eye bars, gives unobstructed access to the entire visual field, and allows the animal to be placed repeatedly in the stereotaxic apparatus without significant error). After the cap was removed from the cylinder a hole was drilled through the acrylic layer and bone and the dura left intact. After all surgical procedures were completed the administration of halothane was discontinued. Anesthesia was maintained by a 7 : 3 mixture of nitrous oxide and oxygen for the duration of the recording session. The animal was immobilized with an intravenous infusion of pancuronium bromide (Pavulon) in saline. Paralysis was maintained with an infusion rate of 0.08 mg $\times$ kg^{-1} $\times$ h^{-1}. Body temperature was maintained at 37–38° C with a heating pad, and the respiratory rate was adjusted to give an end-tidal carbon dioxide level of about 4%. The pupils were dilated with cyclopentolate (Cyclogyl, 1%) and the corneas were covered with contact lenses selected to focus the eyes on the 57 cm distant rear-projection tangent screen.

Recording sessions generally continued for 12–36 h. One hour before the end of the experiment, the paralytic agent was discontinued. The cylinder was washed out and filled with saline and the animal allowed to recover. Usually within 3 h the animal was alert and active in its home cage. At least 2 days separated successive recording sessions.

The data reported here were collected from the same population of neurons that were described in a previous study (Albright et al. 1984).

Recording

Varnish-coated tungsten microelectrodes with exposed tips of 10 μm or less were used to record extracellular potentials from single isolated neurons. In one animal, recordings were confined to the cortex representing an area of the visual field within approximately 10° of the fovea. In the other three animals recordings extended into cortex representing visual field eccentricities ranging from approximately 5° to 25°.

Cells in MT were sampled on long microelectrode penetrations that were made either nearly normal or nearly tangential to the cortical surface. For the tangential penetrations, the electrodes were angled down the posterior bank of the superior temporal sulcus (STS), tilted posteriorally 40° from vertical in the parasagittal plane. These penetrations entered MT at its posterior dorsolateral border after passing through several millimeters of visual cortex posterior to MT. For the penetrations nearly normal to the surface, the electrodes were tilted anteriorally 30° from vertical in the opposite direction from the angles used for the tangential penetrations. These penetrations passed through the lateral surface of area 7 and through the anterior bank of STS before reaching area MT (see Fig. 1, Albright et al. 1984).

Single cells were recorded at closely spaced intervals through the cortex. In the majority of penetrations receptive field size and location were determined for cells isolated at 50 μm intervals, but in two penetrations cells were isolated at 100 μm intervals in order to sample from a larger area of cortex. On the rare occasions that a single cell could not be adequately isolated, the receptive field size and location of a small group of cells were determined. We also measured the preferred direction of motion for every cell. The columnar arrangement of the directionally selective cells has been reported previously (Albright et al. 1984).

Visual stimuli

Visual stimuli were presented on a 60° $\times$ 60° rear-projection tangent screen with a background luminance of 2 cd/m^2. Stimulus intensity was approximately 1.5 log units above background intensity. Receptive field size and location were determined for each cell by use of a hand-held tungsten filament projector and an audio monitor of cellular activity. These receptive field measurements were made in a manner similar to the "minimum response field" method (Barlow et al. 1967) and the criteria were applied consistently by the same experimenters for all cells in the sample. In a few cases the receptive fields were also mapped with a moving stimulus under the control of a PDP-11/34A computer and an X/Y-

mirror optical system. As indicated in the Results, hand-plotted receptive field dimensions bore a highly consistent relationship to those obtained from computer-plotted fields.

Stimuli consisted of moving white or colored spots or elongated slits. The optimal stimulus size, contrast, direction, and speed of motion were estimated for each isolated unit, and this optimal stimulus was then used to measure receptive field size and location through the eye contralateral to the recording site.

Histology

Several days after the last recording session, the animal was anesthetized with an overdose of sodium pentobarbital and perfused with saline followed by 10% buffered formalin. The brain was then photographed and placed in sucrose formalin until it sank. In the three animals in which area MT was entered by electrodes aimed to be normal to the cortical surface, the brains were sectioned at an angle of 30° forward from the frontal plane. In the fourth animal, the brain was sectioned in the parasagittal plane. Sections were cut at 33 μm and alternate sections were stained with cresyl violet and either a modified Heidenhain myelin stain (Gattass and Gross 1981) or a silver based myelin stain (Gallyas 1969). The position of area MT within the superior temporal sulcus was determined from the myeloarchitectonic boundaries seen in serial sections (Ungerleider and Mishkin 1979; Gattass and Gross 1981; Van Essen et al. 1981). The locations of all recording sites were determined on the bases of several small electrolytic lesions (4 μA, 20 s) made on each penetration. All electrode penetrations were reconstructed from serial sections and the laminar position of each recording site was established as well as its position relative to the myeloarchitectonic borders of MT.

The angle of each penetration relative to the cortical surface was calculated from the penetration angles measured in both the plane of section and in the plane orthogonal to the plane of section according to a method described previously (Albright et al. 1984).

Results

A total of 521 single units in area MT were studied on 20 penetrations in four *Macaca fascicularis*. The high incidence of direction selectivity and notable lack of form or color selectivity among the neurons in this sample has been previously reported (Albright et al. 1984) and is in accordance with the results of other studies (e.g., Zeki 1974; Maunsell and Van Essen 1983; Albright 1984). The overall visual topography of MT was found to conform to that previously reported (Gattass and Gross 1981; Van Essen et al. 1981).

Receptive field size

Receptive field size, measured as the square root of receptive field area, was found to increase as a linear function of eccentricity. A plot of receptive field size vs. eccentricity is shown in Fig. 1A along with the regression line:

$$\text{RF Size} = 1.04° + 0.61\ \text{Ecc}$$

The slope of this regression line for single units was significantly smaller than that obtained from multi-unit recordings (0.91) by Gattass and Gross ($t = 8.24$; $df = 566$; $p < 0.001$), but the y-intercepts were similar. For comparison, receptive field size measurements for single units in V1 obtained from different laboratories (Hubel and Wiesel 1974b; Dow et al. 1981) are shown in Fig. 1B. At a given eccentricity, single-unit receptive fields in MT were about ten times larger than those reported for V1. Gattass and Gross (1981) observed the same 10 : 1 ratio when comparing multi-unit receptive field sizes in MT and V1.

Receptive field scatter

In any sensory area, the receptive field location in a vertical column of cells typically exhibits jitter or scatter about the mean from one cell to the next. This leads to the appearance of local disorder in the visual field map in recordings from successive cells on tangential penetrations. Although scatter along vertical penetrations has been measured directly in V1, MT's relative inaccessibility made precisely vertical penetrations impossible. Consequently, as an alternative, we measured the scatter from the mean receptive field trajectory of cells recorded on non-vertical penetrations.

On typical penetrations through MT, receptive fields appeared to move systematically through the visual field, but from one cell to the next there was some deviation from the average receptive field trajectory. To measure these deviations, it was first necessary to calculate the average trajectory. The visuotopic map in MT, like that in V1, can be roughly approximated by a complex logarithmic transform of the visual field coordinates (Schwartz 1980). Polar coordinates in the visual field are thus mapped to a roughly rectilinear system in the cortex. Long penetrations through a map of this sort are expected to yield curved or spiral trajectories of receptive field centers. In fact, the receptive field sequence or trajectory of only one of our penetrations was curved, whereas all other sequences could be fitted very well by a straight line, i.e. the sequences progressed along a straight line across the visual field. These straight-line sequences were all from penetrations of less than 3 mm in length (measured parallel to the cortical surface), implying that over short distances receptive field sequences are unaffected by the global form of the cortical visuotopic map. The single curved trajectory was from a penetration of 4.3 mm in length; however, we found that even this curved trajectory could be fitted reasonably well by two straight lines if the penetration was

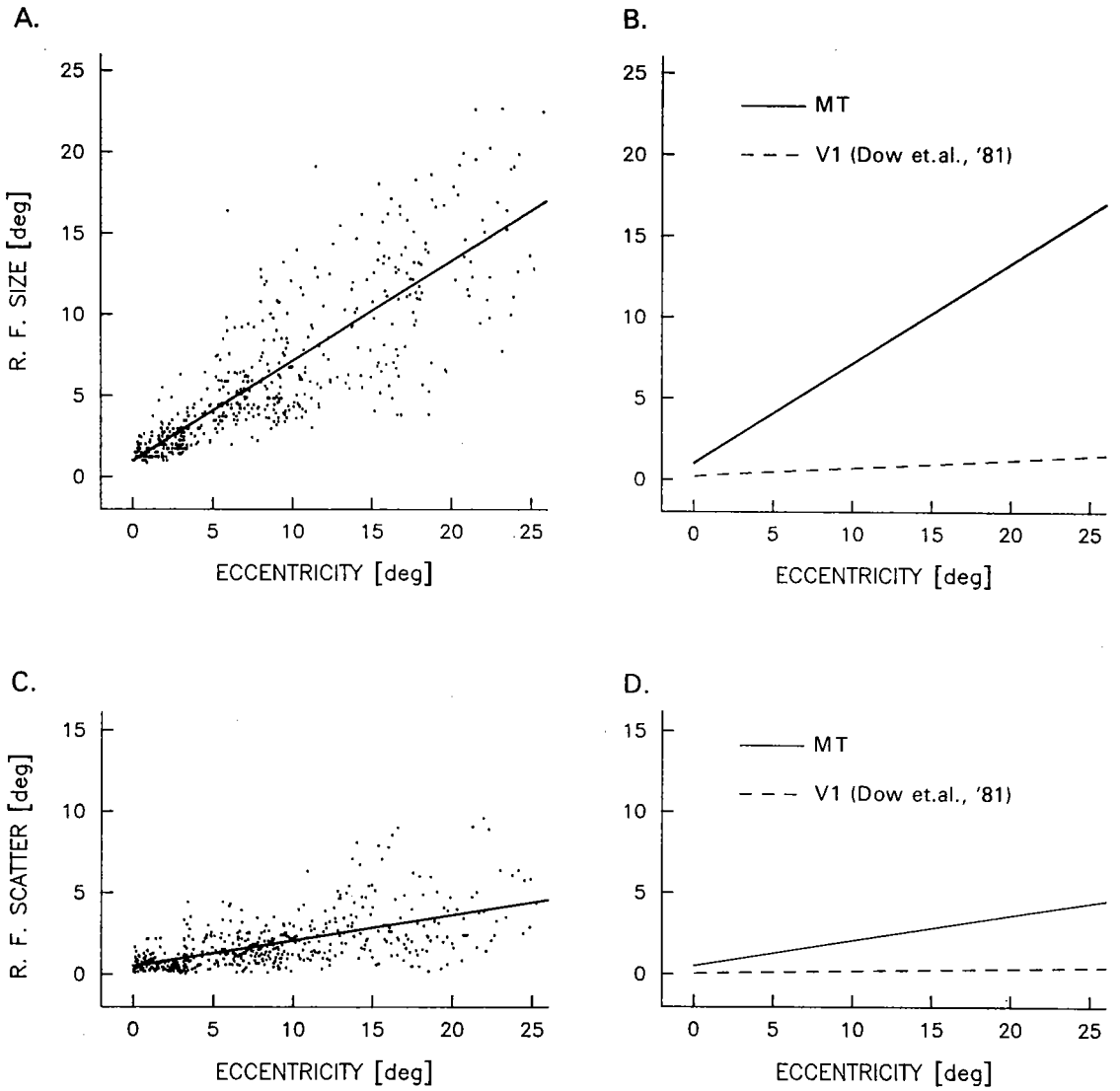

Fig. 1. **A** Receptive field size [sqrt (area)] as a function of eccentricity for single neurons in area MT. N = 514. The regression line for MT (solid line) is given by the equation: RF Size = 1.04° + 0.61 Ecc. **B** The function for single-unit receptive field size in MT (solid line) is plotted for comparison with that obtained previously from V1 by Dow et al. (1981). [The receptive field size function reported by Dow et al. is based on both their own data and that of Hubel and Wiesel (1974b).] Receptive fields in MT are about ten times larger than those in V1 at all eccentricities. **C** Receptive field scatter (magnitude of receptive field center deviation from expected position – see Fig. 2) as a function of eccentricity for single neurons in area MT. N = 514. The regression line for MT (solid line) is given by the equation: RF Scatter = 0.51° + 0.16 Ecc. **D** The function for single-unit receptive field scatter in MT (solid line) is plotted for comparison with that obtained previously from V1 by Dow et al. (1981). Receptive field scatter in MT is about ten times larger than that in V1 at all eccentricities. Furthermore, as in V1, receptive field scatter in MT is roughly one-third as large as receptive field size

divided into two parts. A linear regression was therefore calculated for all 19 short sequences and the two sequences forming parts of the longer penetration. The regression was calculated separately for changes in the X and Y coordinates of the receptive field centers along each sequence. Examples are shown in Figs. 2 and 3.

The 21 sequences used in this analysis ranged in length from 500 μm up to 2900 μm with a mean of 1507 μm. Measurements of receptive field position were typically made at 50 μm intervals along each sequence; there were, on the average, 24 measurements per sequence. The "goodness of fit" for each of our regression lines was evaluated by the size of the mean of the squared residuals. The latter ranged from 0.02° to 19.83° with a mean of 3.96° and were also positively correlated with the mean eccentricity of each sequence (r = 0.65), which is exactly what

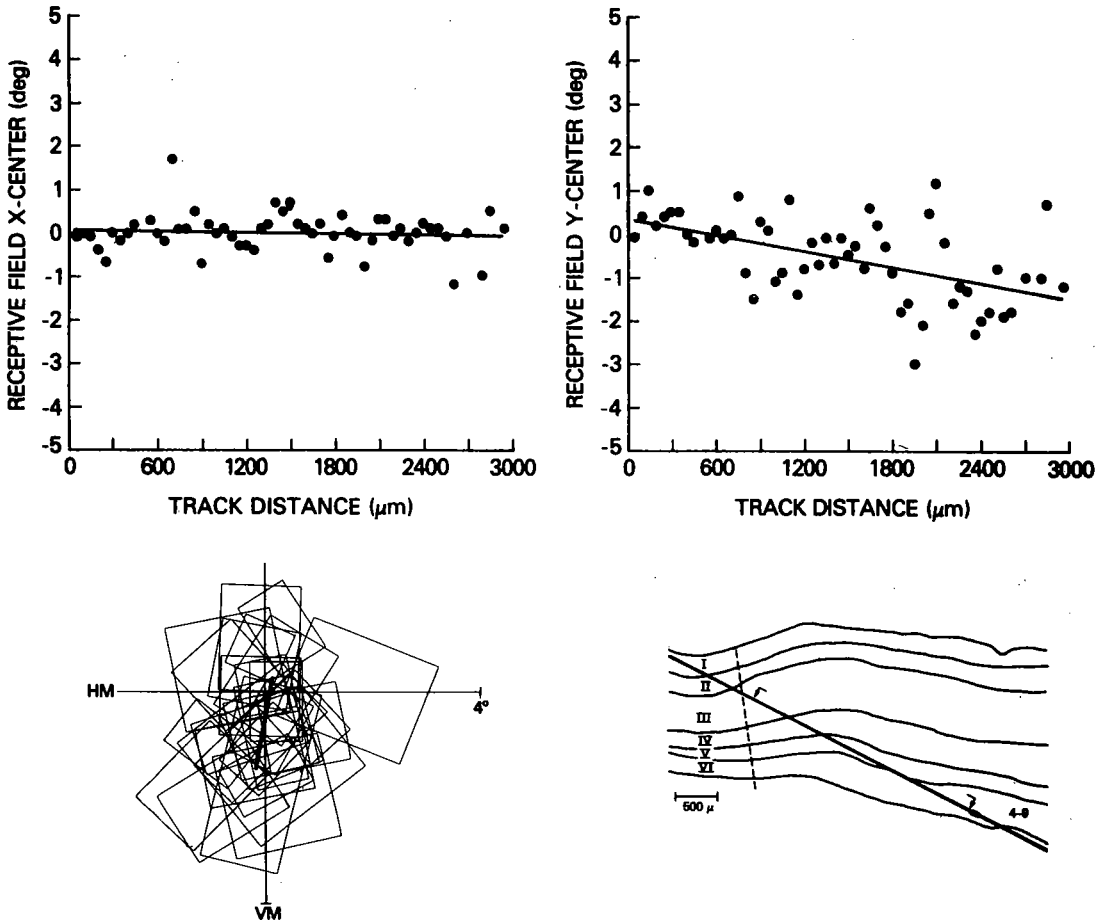

Fig. 2. Analysis of receptive field scatter along a penetration through the foveal representation of MT. Top: A linear regression (solid lines) was computed for both the X- and Y-coordinates of the field centers and provided an excellent fit, on this and other penetrations, for distances up to 3 mm parallel to the cortical surface. The slopes of regression lines were used to calculate magnification factor (see Fig. 4A) and the deviations of field centers from the regression lines were used to calculate scatter (see Fig. 1C). Bottom: Receptive fields of neurons recorded along the penetration (reconstruction on right). For clarity, only every other field is shown. The solid line indicates average trajectory of the field centers

we would expect if scatter in receptive field position is proportional to eccentricity (see below). We did not detect any significant skew in the size of residuals along any of the sequences. For comparison, we also calculated the linear regression based on the eccentricity and polar angle of the receptive field centers, but the regression lines did not fit as well as those based on the cartesian coordinates of the centers.

Once the average trajectories were calculated, scatter could be derived from the X and Y deviations of individual receptive fields using the formula:

$$\text{Scatter } X_iY_i = \text{sqrt } (X_i^2 + Y_i^2),$$

where X_i and Y_i are the individual deviations from the X and Y regression lines. The scatter at different eccentricities is shown in Fig. 1C. The equation of the line describing the relationship is:

$$\text{RF Scatter} = 0.51° + 0.16 \text{ Ecc}$$

This function is analogous to that obtained by Dow et al. (1981) from scatter of receptive field centers along vertical penetrations at different eccentricities in V1[1]. Figure 1D shows that receptive field scatter in MT was about ten times greater than in V1 at comparable eccentricities. However, in both MT (present results) and V1 (Dow et al. 1981), scatter was equal to about one-third of the receptive field size. Thus, the ratio of receptive field scatter to size is comparable in the two

1 Because it is derived from the regression of receptive field scatter onto eccentricity, our best estimate of scatter is approximately $\Sigma r_i/N$ for each eccentricity, where r_i equals the vector distance between the observed and the expected receptive field center for the i^{th} unit. The estimate used by Dow et al. (1981) for V1 is:

$$\text{sqrt } (\Sigma r_i^2/N)$$

Our measure is a good approximation to that used by Dow et al. since the values of r_i are small

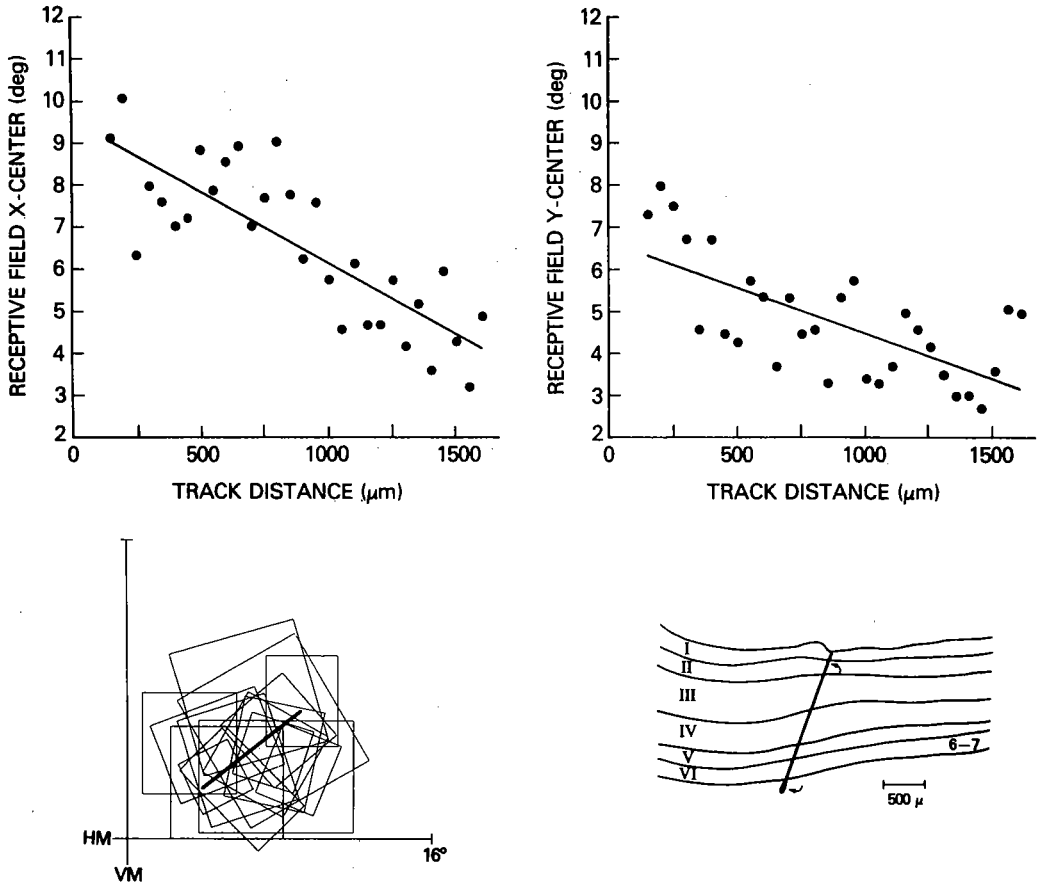

Fig. 3. Analysis of receptive field scatter along a penetration through the parafoveal representation of MT. Top: Progressions of X- and Y-coordinates of field centers. Bottom: Receptive fields of neurons recorded along the penetration shown at right. See also legend to Figure 2

areas even though the absolute scatter is much greater in MT.

Magnification factor

Magnification factor is defined as the cortical distance corresponding to one degree of separation in the visual field. The receptive field trajectories derived for the computation of scatter could also be used to compute the magnification factor in MT. To do so, it was first necessary to correct the electrode tract measurements for distance measured parallel to the cortical surface; thus, all tract distances were multiplied by the sine of the angle of the penetration relative to the radial cell columns (Albright et al. 1984). The rate of change of receptive field location on each trajectory was then expressed as a function of cortical distance measured parallel to the surface (i.e., degrees/mm). The reciprocal of these values, magnification factor (mm/degree), as a function of average receptive field eccentricity is shown for 21 receptive field sequences in Fig. 4A.

Because the number of magnification factor estimates available from our data was small, we combined our data with those of Gattass and Gross (1981), who derived magnification factor estimates from MT by making a large number of penetrations in one animal and comparing receptive field locations across the different penetrations. They have kindly made their data available to us, and these are plotted along with the data of the present study in Fig. 4A[2]. The two sets of data are in close agreement, and the power functions that best fitted the two sets are not significantly different ($t = 1.55$; $df = 104$; $p > 0.1$). The function that best fits the combined data set is:

$$MF = 1.14\ Ecc^{-0.76}$$

Magnification factor in MT reaches nearly 2.0 mm/deg at the representation of 0.5° eccentricity. It drops off rapidly in the parafoveal region, reaching

2 The magnification factor function reported for MT by Gattass and Gross (1981) was, in fact, not the best fit to their data. The corrected function is: $MF = 1.19\ Ecc^{-0.74}$

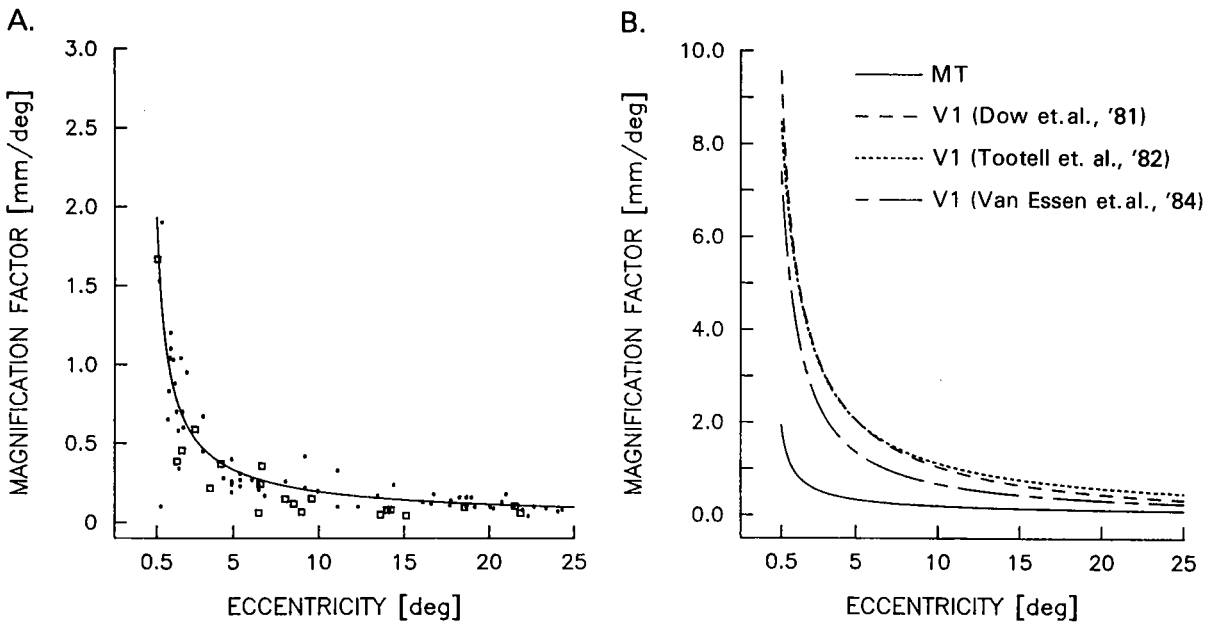

Fig. 4. A Cortical magnification factor as a function of eccentricity in area MT. Measurements of magnification factor obtained from the present study (rectangles, N = 21) have been combined with those from Gattass and Gross (1981) (dots, N = 87). The two sets of data are in close agreement and the power functions that best fit the two sets independently are not significantly different. The power function that best fits the combined data set (solid line) is: MF = 1.14 $Ecc^{-0.76}$. **B** The function for cortical magnification factor in MT (solid line) is plotted for comparison with functions obtained previously for V1 by different laboratories using different techniques (electrophysiology: Dow et al. 1981; Van Essen et al. 1984; 2-deoxyglucose: Tootel et al. 1982). [The magnification factor function reported by Dow et al. (1981) is based on their own data, as well as that of Talbot and Marshall (1941), Daniel and Whitteridge (1961), Hubel and Wiesel (1974b), and Guld and Bertulis (1976).] Note change in scale from that in Fig. 4A. From 0.5° to about 5° eccentricity, magnification factor in MT is about one-fifth that in V1. Beyond 5° however, this ratio increases, reflecting a relatively greater peripheral field expansion in MT

only about 0.2 mm/deg at 10° eccentricity, and drops off much less rapidly beyond about 10°. For comparison, measures of cortical magnification factor in V1 obtained from different laboratories using different techniques (electrophysiology: Dow et al. 1981; Van Essen et al. 1984; 2-deoxyglucose: Tootel et al. 1982) are shown in Fig. 4B. [Magnification factor reported for V1 by Dow et al. (1981) is based on their own data and that of Talbot and Marshall (1941), Daniel and Whitteridge (1961), Hubel and Wiesel (1974b) and Guld and Bertulis (1976)]. Although there is some variability in the V1 measurements, the magnification factor in MT appears to be roughly one-fifth that in V1 for eccentricities up to about 5°. Beyond 5° eccentricity, however, the ratio of magnification factor in MT to that in V1 increases steadily, reaching approximately one-third at 20° eccentricity. Thus, in relation to V1, the peripheral field representation of MT appears to be relatively less compressed than the central field representation.

Point-image size

Point-image size has been defined as the diameter of the region of cortex activated by a single point in the visual field (McIlwain 1976). The point-image size at a given location in the visual field representation of a cortical area is determined by the magnification factor, receptive field size, and scatter in receptive field position at that location. To characterize receptive field size plus scatter in V1, Dow et al. have used a measure termed "aggregate receptive field size", and, for comparison with their results, we have calculated the same measure for MT. The equation for the measure is:

$$\text{Aggregate RF size} = 4 \times \text{sqrt}\,(r^2 + s^2)$$

where r^2 is a measure of single-unit receptive field scatter and s^2 is a measure of single-unit receptive field size. In MT, r is given by the regression equation for scatter as a function of eccentricity, derived previously in the Results. Dow et al. (1981) define s^2 to be equal to (c * RF length * RF width)^2, where c is the proportionality constant that relates the hand-mapped receptive field width to the standard deviation of the computer-mapped receptive field width. This proportionality constant has been reported to be 0.5 for V1, and we obtained a value of 0.49 in MT based on computer- and hand-mapped receptive fields for 45 MT neurons. Thus, on the

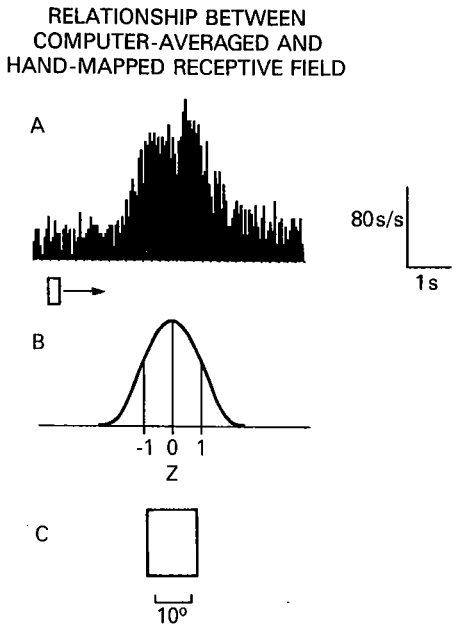

Fig. 5A–C. Top: Response histogram obtained from computer presentation of a moving slit stimulus for a total of five trials. The response is used as an estimate of the sensitivity profile of the receptive field along the axis in which the stimulus was moved. Center: The sensitivity profile has been approximated by a Gaussian function. The width of the hand-plotted field (Bottom) was about one standard deviation to each side of the peak of the response sensitivity profile. This was true for most MT neurons that were tested with both computer and hand presentation of stimuli. The "proportionality constant" used to compute aggregate field size is, thus, about 0.5, reflecting the ratio of the standard deviation of the computer plotted sensitivity profile to the hand-plotted field width

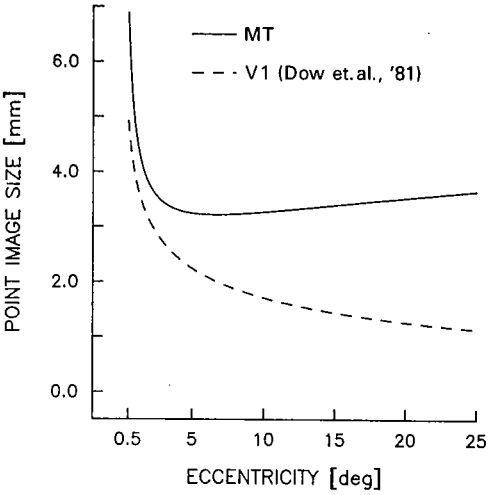

Fig. 6. Point-image size as a function of eccentricity for areas MT (present study) and V1 (Dow et al. 1981). Point-image size is an estimate of the diameter of the cortical surface activated by a single point in the visual field (McIlwain 1976). We have calculated this measure from MT single-unit receptive field size, scatter and magnification factor using a method identical to that previously used in V1 (Dow et al. 1981): Point-image size = $4 \times \text{sqrt}(\text{size}^2 + \text{scatter}^2) \times$ magnification factor. The two functions become increasingly divergent at greater eccentricities due to relatively less peripheral visual field compression in MT. (cf. magnification factor, Fig. 4B)

average, roughly one-half of the width of a hand-mapped receptive field is equal to one standard deviation of the computer-mapped receptive field profile. An example of the computer- and hand-mapped receptive fields for one cell is shown in Fig. 5. Finally, a factor of four is used for calculation of the aggregate field size in order to include two standard deviations of the aggregate receptive field spread to each side of the aggregate field center. In order to compare our results with those of Dow et al., we included these two standard deviations of aggregate receptive field spread to each side of the aggregate receptive field centers, although it might be argued that this yields an overly large estimate of aggregate field size.

After computing the aggregate receptive field size at each eccentricity, the point-image can be derived from the product of aggregate field size and magnification factor. Figure 6 shows the point-image size in MT and, for comparison, the results from Dow et al. (1981) in V1. Van Essen et al. (1984) also computed the point-image size for V1, and obtained values that were significantly smaller than those reported by Dow et al. However, Van Essen et al. used multi-unit receptive field size as an estimate of the aggregate field size, and, therefore, their results are not strictly comparable to either those of Dow et al. or the present study.

Although magnification factor is much smaller in MT than in V1, receptive field size in MT is correspondingly larger, so that the point-image size in the two areas is comparable, especially within the central 5°. Beyond about 5°, magnification factor decreases more slowly in MT than in V1, and consequently the point-image size in MT appears about twice that in V1.

Discussion

Although MT is much smaller than V1 and has much larger receptive fields, there are a number of striking similarities between the two areas. In both V1 and MT there is an orderly representation of the visual field, with scatter approximately equal to about one-third of the size of the receptive fields. Furthermore, the point-image size in MT is comparable to that in V1 for the representation of the central visual field and even appears somewhat larger than that in V1 for the representation of the peripheral visual field.

Maunsell and Van Essen (1986) have pointed out that absolute measures of point-image size can vary considerably across different studies. It is, therefore, reassuring that, using different techniques and measures, they also have found point-image size in MT to be somewhat larger than that in V1. Thus, taking our results and theirs together, it is probably safe to conclude that the point-image size in MT is at least no *smaller* than that in V1, which is itself a surprising result given that MT is smaller than V1 by at least a factor of 10.

Visuotopic organization of MT

The results of the present study indicate that the visuotopic organization of MT is highly orderly, at least over distances up to 3 mm. These results confirm the observations made by Gattass and Gross (1981). Yet, it has previously been reported that the visuotopic organization of MT is crude at best (Dubner and Zeki 1971; Van Essen et al. 1981). One factor that may contribute to this apparent discrepancy is that the visuotopic organization of MT is locally orderly but globally distorted. Recent studies by Desimone and Ungerleider (1986) and Maunsell and Van Essen (1986) have found that, in some animals, the global visual field representation in MT can be highly distorted. For example, in one case, Desimone and Ungerleider found that although MT receptive fields progressed in an orderly manner on a local scale, the overall representation of the horizontal meridian was roughly U-shaped. Since the mean length of our receptive field trajectories is only 1.5 mm, it is not surprising that we could not detect such distortions in the present study.

A second issue that can be addressed by our results is the size of MT. A number of studies have indicated that the full visual field representation in MT of the macaque occupies approximately 70 mm^2 (Ungerleider and Mishkin 1979; Gattass and Gross 1981; Weller and Kaas 1983; Ungerleider and Desimone 1986a; Desimone and Ungerleider 1986). The representation of the central visual field in MT occupies a heavily myelinated zone in STS, while at least part of the peripheral field appears to lie outside of this heavily myelinated zone (Desimone and Ungerleider 1986). By integrating the areal magnification factor from 0.5° eccentricity to 90° eccentricity, we have arrived at a size of 61.5 mm^2 for MT, which is consistent with these earlier estimates. By contrast, Van Essen et al. (1981) reported that MT occupies only 33 mm^2, about half the size found in the present study and others. Part of the discrepancy may be due to the fact that Van Essen et al. considered the complete visual field representation of MT to be confined to the heavily myelinated zone, and part may be due to the small size of the macaques used in their study (see Maunsell and Van Essen 1986 and Ungerleider and Desimone 1986b for a more complete discussion of these points). More recently, Maunsell and Van Essen (1986) have measured the size of the heavily myelinated zone in STS to be 39 mm^2 while they calculated the size of the visual field representation to be 60–80 mm^2 based on the magnification factor in MT. While the difference in size between the heavily myelinated zone and the visual field representation supports the findings of earlier studies that MT extends beyond the heavily myelinated zone, Maunsell and Van Essen conclude that MT is confined to the heavily myelinated zone, arguing that possible differences between the magnifications for the upper and lower visual field representations of MT may inflate any estimate of its size based on magnification factor.

Modules in MT

We recently reported that, within the horizontal dimension of MT, the directional preferences of successively recorded cells changed systematically by small increments or, occasionally, by 180° (Albright et al. 1981, 1984). The results suggested that "axis-of-motion" (analogous to stimulus orientation) columns were organized in systematic arrays across MT. The scale of the columnar system was very similar to that for orientation in V1, in that 180° of axis of motion was represented in a minimum of about 400–500 μm, which is about the same size as the representation of 180° of orientation in V1 (Hubel and Wiesel 1974a; but see Blasdel and Salama 1986). From metabolic mapping experiments, Burkhalter et al. (1981) have also found evidence for axis-of-motion columns in MT. Although 500 μm seems large when compared to the size of MT, the point-image size in MT is sufficiently large to encompass at least one complete set of axis-of-motion columns, or motion "module", at all eccentricities. In the foveal representation of MT, a single point activates several modules, which may underlie the ability to make fine motion discriminations in the foveal field. In fact, in the central visual field, a single point should activate about the same number of motion modules in MT as of orientation modules in V1 because the point-image as well as the module size are comparable across these areas. Thus, in spite of its small size, MT appears to contain at least as much neural machinery for processing the information from a given point in the visual field as does V1.

The fact that the cortical region activated by a single point in the visual field encompasses a larger proportion of the visual field representation in MT than in V1 suggests that processing power in MT is maintained at the expense of a loss of spatial resolution. Two closely spaced moving stimuli in the visual field may result in completely separate foci of activity in V1 but a common focus of activity in MT. In fact, two stimuli that activate different populations of neurons in V1 may both fall within the same receptive field of a cell in MT. How the visual system compensates for such a loss of resolution is not known. One possibility is that, due to receptive field scatter, two spatially separate stimuli will always fall within two partially non-overlapping sets of receptive fields, and this difference is decoded by the visual system (McIlwain 1976). Another possibility is that, in the behaving animal, spatial resolution is achieved by directed visual attention. In area V4 and in inferior temporal cortex, it has been found that when an animal attends to stimuli at one location within the receptive field of a cell, responses of the cell to stimuli at other locations are attenuated (Moran and Desimone 1985). If such an attention mechanism also operates in MT, spatial resolution in MT would be limited only by the size of the focus of attention.

Acknowledgements. We wish to thank C. Gross for advice, assistance and support on all aspects of these experiments; T. Farris for histology; C. Colby, J. Maunsell, M. Mishkin and H. Rodman for comments on the manuscript; M. Rosengarten and D. Flowers for typing.

This study was supported by National Institutes of Health grant MH-19420 and National Science Foundation grant BNS-8200806.

References

Albright TD (1984) Direction and orientation selectivity of neurons in visual area MT of the macaque. J Neurophysiol 52: 1106–1130

Albright TD, Desimone R (1984) Precision of visuotopic organization of area MT in the macaque. Neurosci Abstr 10: 474

Albright TD, Desimone R, Gross CG (1981) Organization of directionally selective cells in area MT of macaques. Neurosci Abstr 7: 832

Albright TD, Desimone R, Gross CG (1984) Columnar organization of directionally selective cells in visual area MT of the macaque. J Neurophysiol 51: 16–31

Allman JM, Kaas JH (1971) A representation of the visual field in the caudal third of the middle temporal gyrus of the owl monkey (*Aotus trivirgatus*). Brain Res 31: 85–105

Baker JF, Petersen SE, Newsome WT, Allman JM (1981) Visual response properties of neurons in four extrastriate visual areas of the owl monkey (*Aotus trivirgatus*): a quantitative comparison of the medial, dorsomedial, dorsolateral, and middle temporal areas. J Neurophysiol 45: 397–416

Barlow HB, Blakemore C, Pettigrew JD (1967) The neural mechanism of binocular depth discrimination. J Physiol (Lond) 198: 327–342

Blasdel GG, Salama G (1986) Voltage sensitive dyes reveal a modular organization in monkey striate cortex. Nature 321: 579–585

Burkhalter A, Van Essen DC, Maunsell JHR (1981) Patterns of 2-deoxyglucose labeling in extrastriate visual cortex of unstimulated and unidirectionally stimulated macaque monkeys. Neurosci Abstr 7: 172

Daniel PM, Whitteridge D (1961) The representation of the visual field in the cerebral cortex in monkeys. J Physiol (Lond) 159: 302–321

Desimone R, Ungerleider LG (1986) Multiple visual areas in the caudal superior temporal sulcus of the macaque. J Comp Neurol 248: 164–189

Dow BM, Snyder AZ, Vautin RG, Bauer R (1981) Magnification factor and receptive field size in foveal striate cortex of the monkey. Exp Brain Res 44: 213–228

Dubner R, Zeki SM (1971) Response properties and receptive fields of cells in an anatomically defined region of the superior temporal sulcus in the monkey. Brain Res 35: 528–532

Gallyas F (1969) Silver staining of myelin by means of physical development. Orvostucomany 20: 433–489

Gattass R, Gross CG (1981) Visual topography of the striate projection zone in the posterior superior temporal sulcus (MT) of the macaque. J Neurophysiol 46: 621–637

Guld C, Bertulis A (1976) Representation of fovea in the striate cortex of vervet monkey, *Cercopithecus aethiops pygerythrus*. Vision Res 16: 629–631

Hubel DH, Wiesel TN (1963) Shape and arrangement of columns in cat's striate cortex. J Physiol (Lond) 165: 559–568

Hubel DH, Wiesel TN (1974a) Sequence regularity and geometry of orientation columns in the monkey striate cortex. J Comp Neurol 158: 267–294

Hubel DH, Wiesel TN (1974b) Uniformity of monkey striate cortex: a parallel relationship between field size, scatter and magnification factor. J Comp Neurol 158: 295–306

Livingstone MS, Hubel DH (1984) Anatomy and physiology of a color system in the primate visual cortex. J Neurosci 4: 309–356

Lund JS, Lund RD, Hendrickson AE, Bunt AH, Fuchs AF (1975) The origin of efferent pathways from the primary visual cortex, area 17, of the macaque monkey as shown by retrograde transport of horseradish peroxidase. J Comp Neurol 164: 287–304

Maunsell JHR, Van Essen DC (1983) Functional properties of neurons in middle temporal visual area of the macaque monkey. I. Selectivity for stimulus direction, speed, and orientation. J Neurophysiol 49: 1127–1147

Maunsell JHR, Van Essen DC (1986) The topographic organization of the middle temporal visual area in the macaque monkey and its relationship to callosal connections and myeloarchitectonic boundaries. (in press)

McIlwain JT (1976) Large receptive fields and spatial transformations in the visual system. Int Rev Physiol 10: 2563–2586

Moran J, Desimone R (1985) Selective attention gates visual processing in the extrastriate cortex. Science 229: 782–784

Mountcastle VB (1957) Modality and topographic properties of single neurons of cat's somatic sensory cortex. J Neurophysiol 20: 408–434

Schwartz EL (1980) Computational anatomy and functional architecture of striate cortex: a spatial mapping approach to perceptual coding. Vision Res 20: 645–669

Talbot SA, Marshall DW (1941) Physiological studies on neural mechanisms of visual localization and discrimination. Am J Ophthalmol 24: 1255–1263

Tootel RBH, Silverman MS, Switkes E, DeValois RL (1982) Deoxyglucose analysis of retinotopic organization in primate striate cortex. Science 218: 902–904

Ungerleider LG, Desimone R (1986a) Cortical connections of visual area MT in the macaque. J Comp Neurol 248: 190–222

Ungerleider LG, Desimone R (1986b) Projections to the superior temporal sulcus from the central and peripheral field representations of V1 and V2. J Comp Neurol 248: 147–163

Ungerleider L, Mishkin M (1979) The striate projection zone in the superior temporal sulcus of *Macaca mulatta*: location and topographic organization. J Comp Neurol 188: 347–366

Van Essen DC, Maunsell JHR, Bixby JL (1981) The middle temporal visual area in the macaque: myeloarchitecture, connections, functional properties and topographic organization. J Comp Neurol 199: 293–326

Van Essen DC, Newsome WT, Maunsell JHR (1984) The visual field representation in striate cortex of the macaque monkey: asymmetries, anisotropies, and individual variability. Vision Res 24: 429–448

Weller RE, Kaas JH (1983) Retinotopic patterns of connections of area 17 with visual areas V-II and MT in macaque monkeys. J Comp Neurol 220: 253–279

Zeki SM (1974) Functional organization of a visual area in the posterior bank of the superior temporal sulcus of the rhesus monkey. J Physiol (Lond) 236: 549–573

Received January 15, 1986 / Accepted October 22, 1986